Available online at www.CivileJournal.org

Civil Engineering Journal

(E-ISSN: 2476-3055; ISSN: 2676-6957)

Vol. 10, No. 06, June, 2024

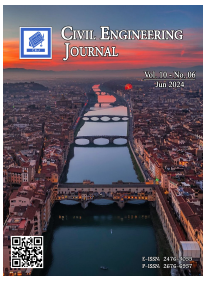

Quantitative Monitoring of Coastal Erosion and Changes Using Remote Sensing in a Mediterranean Delta

Khaled Mahmoud Abdel Aziz [1, 2*]

[1] *Department of Civil Engineering, College of Engineering in Al-Kharj, Prince Sattam Bin Abdulaziz University, Al-Kharj 11942, Saudi Arabia.*

[2] *Geomatics Engineering Department, Faculty of Engineering at Shoubra, Benha University, Cairo, Egypt.*

Received 02 February 2024; Revised 04 May 2024; Accepted 11 May 2024; Published 01 June 2024

Abstract

The morphology of coastal regions is continually changing because of both natural and human factors. Monitoring and understanding these changes are essential for efficient coastal management and sustainable development. To protect and develop beaches, quantitative monitoring of coastal changes is crucial. According to this study, there is a persistent erosion issue with the shoreline of the Rosetta region in Egypt. Over the previous century, there has been noticeable erosion. This is mostly because of the Aswan High Dam, which was built in 1964 and decreased runoff and sediment flow. Five Landsat images spanning the years 1980–2023 were utilized in this study. The Nile Delta would be eroding at an alarming rate if action were not taken due to coastal erosion, which is made worse by sea level rise. Our study's primary goal is to evaluate the shoreline of the Rosetta region and identify rates of erosion and accretion as well as patterns of accumulation and erosion using a combination of statistical analysis of the coastline using DSAS software and remote sensing techniques. It also seeks to pinpoint hotspots that require security. In this study, the Shoreline Linear Regression Rate (LRR), End Point Rate (EPR), Shoreline Change Envelope (SCE), and Net Shoreline Movement (NSM) were determined by creating cross-sections perpendicular to the baseline using the Digital Shoreline Analysis System (DSAS). According to the analysis of coastal change, the periods with the highest levels of erosion were between 1980 and 1990, before the protection of the promontory took place. In addition, the results extracted from this study showed a stabilized shoreline between 2000 and 2023 at the Rosetta Promontory and noticeable erosion in the east and west of the promontory.

Keywords: Shoreline Change; DSAS; Rosetta Promontory; Shoreline Extraction; Remote Sensing; ArcGIS; Shore Protection Authority; EPR; NSM; ESC; LRR.

1. Introduction

The world's coasts are constantly changing and becoming more susceptible and vulnerable because of a variety of reasons, most notably climate change and human activity. Coastal areas globally are under significant strain, as seen by recent catastrophic climatic occurrences witnessed in many parts of the world [1]. For integrated coastal area management, coastline change analysis and forecasting are essential, and field and aerial surveys are usually used for this [2]. Ground measurements, aerial photogrammetry, and remote sensing analysis utilizing satellite pictures can be used for drawing shoreline maps [3]. Satellite imaging is now being used to analyze coastal change as a result of technological advancements [4]. Satellite imagery has been frequently employed in studies of coastal change monitoring and analysis, as well as erosion prediction. Landsat, Quickbird, Allos, SPOT, IKONOS, and other satellite data are often utilized in coastal change monitoring and analysis [5].

* Corresponding author: khaled.mahmoud@feng.bu.edu.eg

http://dx.doi.org/10.28991/CEJ-2024-010-06-08

Coastal zones are now experiencing shoreline alterations because of natural and manmade causes. Erosion and accretion will have an impact on the shoreline's physical environment. As a result, studying shoreline alterations is critical for identifying long-term shift trends. Today's rapid technological advancements have made it easier to examine shoreline alterations. The ability of geographic information systems and remote sensing techniques to collect data, observe, analyze, and predict coastal variations makes them useful instruments for detecting these variations [6].

Numerous natural phenomena, including beach erosion, flooding, and sea level rise, cause changes to coastlines. Shoreline morphology has been altered recently by human activity, coastal processes, and climate change. In recent years, one of the most significant environmental issues has been the shifting position of the coast. According to research, the majority of the world's coasts are receding at a pace of between 1 cm and 10 m per year due to erosion. Geographic Information Systems and remote sensing have made it easier to map the spatial and temporal changes in the coastal environment. To assist decision-makers in making wise choices, maps can show the regional variations in coastal erosion and accretion as well as forecast future conditions [7]. The most usable of medium-resolution images for researching the dynamics of coastal areas is the Landsat image collection obtained by the TM and ETM + sensors on the Landsat 5, 7, 8, and 9 series. Because Landsat data sets have covered the entire planet continuously for more than 50 years, they are extremely valuable for large-scale studies [8].

Half of the shoreline of the Nile Delta was eroded, and the other half was accreted between 1945 and 2015. There are five different types of shoreline changes along the Nile Delta coast: (1) somewhat stable (51% of the coast); (2) shoreline change from 2.90 to 7.0 m/year (33% of the coast); (3) shoreline change from 7.0 to 29.0 m/year (12% of the coast); (4) shoreline change from 29.0 to 57.0 m/year (3% of the coast); and (5) shoreline change greater than 57.0 m/year, which only occurred on Rosetta Promontory [7].

Egypt is one of the top ten nations that climate change and fluctuations in the Mediterranean water level might significantly impact. Due to its low height and location on the southern shore of the Mediterranean Sea, Egypt is more vulnerable to the effects of sea level rise. Numerous studies conducted globally have examined the implications of climate change and sea level rise, illustrating the effects of these changes in various parts of the world. Additionally, various studies on coast maintenance have been conducted in Egypt, and the results have shown the financial implications as well as strategies for shielding beaches from impending climate change [9].

Aside from the effects of climate change on coastal regions, other variables such as tides, waves, man-made infrastructure, and the construction of dams—which shield these places by preventing silt from pouring into the sea—may also have noticeable effects. It is important to evaluate each of these factors to track and forecast the changes that are taking place along the shore [9].

The Nile Delta Promontories coastline areas have been negatively impacted by siltation and eroding issues due to the establishment of many entities for water control. Since the construction of the high dam in Aswan in 1964 and other regulating facilities across the Nile, the yearly discharge of sediment has decreased from approximately 120,000,000 tons to almost nothing today. Consequently, the Mediterranean Sea's waves started to alter the areas along the shore. Following the establishment of the high dam in Aswan, the east side of the Rosetta Promontory had an extremely high rate of erosion, up to 80 meters per year. The agricultural lands are at risk due to the shoreline's retreat [10].

The northwest portion of the Nile Delta is home to the Rosetta Promontory. Situated around 60 kilometers east of Alexandria City, it is situated on the eastern end of Abu Qir Bay. Between 500 and 1000 AD, the Canopic and Sebennitic Nile branches were redirected to create the current Rosetta Branch. Rosetta promontory kept accumulating and expanding until the turn of the 20th century, when it had grown to around 14 kilometers in the direction of the sea. Following the completion of the Aswan Low Dam in 1902, the regression process started (see Figure 1). The pace of shoreline change along the Rosetta Promontory was estimated using a variety of methods [11].

The construction of the high dam in Aswan in 1964 caused a large amount of sediment from the river to be trapped beyond it, which accelerated the erosion of the Delta's coastline. The coastline surrounding the Rosetta promontory showed the greatest eroding in the Delta, retreating the coastline at a rate of 137.4 meters every year [12].

The Mediterranean Basin is becoming a hotspot for climate change due to rising sea levels and air temperatures, as reported by Ali et al. (2022) and Torresan et al. (2020)] [13, 14]. Egypt stands out as one of the nations most susceptible to the possible effects of climate change, especially considering the country's unique ecology and economic activity in the northern coastal region. The northern shore of Egypt is particularly vulnerable due to factors such as high population density, fast urbanization, and sea level rise (SLR) [15, 16]. The Nile Delta region is one of the most vulnerable low-lying beaches in the Mediterranean Basin and on Egypt's northern coast due to its high susceptibility to Sea Level Rise (SLR**)** [16-18]. Additionally, the IPCC 2019 [17] stated that 2,660 km^2 of the northern Nile Delta is expected to be flooded by 2100 due to a 0.44 m rise in global mean sea level.

Egypt's coastline extends for 3000 kilometers along the Mediterranean and Red Seas. The 1200-kilometer Mediterranean coastline is distinct from the Red Sea coast due to its unique geology, geomorphology, and geography.

The Mediterranean coast is characterized by deltaic deposits, sand dunes, lagoons, lakes, mud flats, salt marshes, and stony beaches, making it diverse. Major cities such as Matrouh, Alexandria, Rosetta, Damietta, El-Arish, and Port Said are situated along this coast, which is densely populated and developed. Sea-level rise poses a significant threat to the delta, particularly its 250-kilometer shoreline with mountainous terrain. Reports suggest that 31% of the Nile Delta could be submerged with a 100 cm rise in sea levels. Even a one-meter increase in the Mediterranean Sea would have severe consequences for the Nile Delta. The already fragile offshore sand dune belt would be completely eroded by rising sea levels [19].

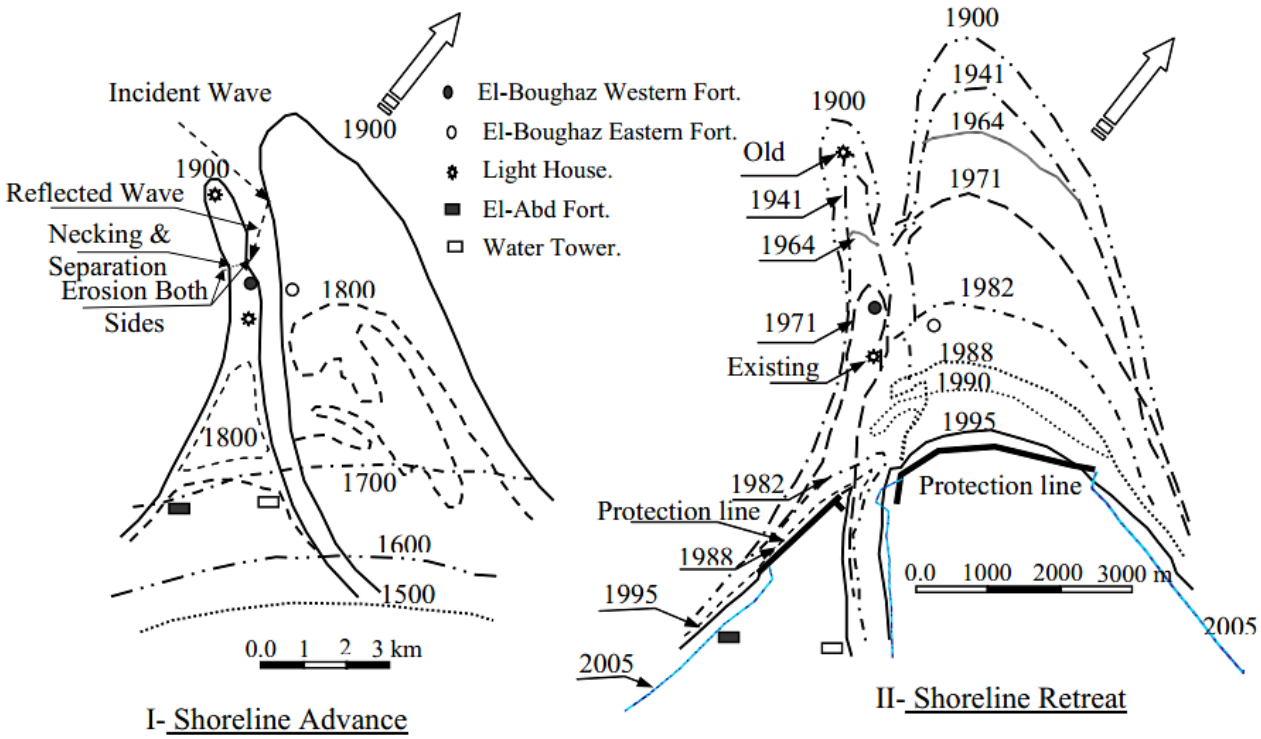

Figure 1. The coastline development of Rosetta Promontory from 1500-2005 [16]

Ghoneim et al. (2015) [12] state that 11 Landsat images acquired at irregular intervals between 1972 and 2012 were analyzed to determine patterns of accretion and erosion along the Rosetta promontory. The shoreline positions that were automatically generated from 11 Landsat photographs were compared with the shoreline locations that were obtained from three high-resolution *QuickBird* and *WorldView2* photos for data validation. The seawall construction was mainly effective in stopping the recession along the promontory's tip, which had lost 10.8 km2 before coastal protection. However, on the shoreline promontory leeside, the construction of the 15 groins has negatively impacted the promontory's coastal morphology and caused a shift from deposition to fast eroding, with certain areas of the shoreline experiencing erosion at a rate of up to 30.8 m/year, which was obtained by analyzing the coastline variation. Portions of the shoreline saw eroding rates between 30.8 and 20 m/year over the after-protection era (1991–2012).

Balbaa et al. (2020) [11] examined how various engineering hard constructions affected the coastal region of Rosetta Promontory and the pattern of shoreline growth along the coastal strip of Rosetta Promontory during a three-decade temporal scale between 1985 and 2015. This study shows that during the past 30 years, erosion has impacted the eastern side of the Rosetta Promontory, with the promontory tip seeing the highest average erosion rate of about -50 m/y. The greatest rate of erosion (about 137 m/y) occurred between 1985 and 1990, before the construction of the eastern revetment. On the other hand, throughout the study, the Western Rosetta Promontory showed an average erosion rate of -15.5 m/y. The Western sector experienced the fastest rate of erosion from 1985 to 1990, before the building of the western barrier. The horizontal coastal retreat at the locations of the eastern and western seawalls has completely stopped since the seawalls were built. On the lee sides of the structures, however, the erosion has moved. The lee sides of the eastern and western seawalls saw erosion rates of around -64 m/y and -20 m/y, respectively.

Masria et al. (2015) [20] present a study that used a multi-time post-classification examination to identify changes in land cover. Coastline locations and coastline frequent variations of the delta shoreline in circumference Rosetta Promontory were extracted from four Landsat images covering the years 1984 to 2014. Four classifications—seawater, developed (urban and agricultural), sabkhas (salt-flat), and undeveloped areas—were selected, and their multi-time variations were evaluated by comparison between the four chosen photos. The coastline was determined by using two various approaches. Firstly, a band 5 histogram threshold is used; secondly, a combination of the band 5 histogram

threshold and 2 band ratios (band 2/band 4 and band 2/band 5). The pace of retreat of the shoreline was found to have decreased by about 70% between 1984 and 2014. Even nevertheless, erosion continues to be severe, with the highest frequency of 37 m per year.

The back-shore surface area and shoreline change rates that occur from these changes, particularly after the building of maritime structures such as groins, detached breakwaters, and seawalls, were calculated by Deabes (2017) [21] using the Geographic Information System (ArcGIS 9.3). A model builder in ArcGIS software was used to create and implement an automated approach, or module, for estimating such changes (rate and area). The coastline's location concerning dominant coastal processes and the analysis of surveys of the beach and nearshore profiles carried out between 1970 and 2010 are used to infer these changes. The findings indicate that the Delta promontories saw the most erosion; the shoreline of Rosetta withdrew (1.6 km) at an average rate of 60 m/yr, losing 6.4 km^2 of back-shore land.

Fouad et al. (2020) [22] use a combination of statistical shoreline analysis utilizing DSAS software and remote sensing techniques to analyze the shoreline zone at Rosetta Promontory to identify rates of corrosion and sedimentation in addition to corrosion/sedimentation modes. It was observed that the rate of erosion was quite high between 1984 and 1995, especially in front of the eastern promontory (127 m/year). Between 1995 and 2004, erosion kept moving until it reached the seawalls erected on the promontory sides. The frequency of corrosion dropped to around 45 meters per year. During the period 2004–2011, erosion was stopped on the frontal walls and redirected to the downdrift, specifically the east side passing the groins (which are constructed to reduce corrosion). On the eastern side of the promontory, the greatest rate of corrosion was 45 meters per year. Between 2011 and 2019, there was a modest rise in the erosion rate, reaching 59 m/year.

Hemida et al. (2023) [23] used content analysis to examine 26 Egyptian coastal vulnerability assessment documents. The results of the study highlight the significance of reassessing assessments of susceptible areas in light of our local environment.

Long-term coastal line monitoring is extremely important. This study has examined earlier research on Rosetta promontory and contrasted its findings with our own. Sustainable development in coastal areas has been impacted by the numerous changes that the coastline has seen in recent decades. Consequently, creating high-precision coastal maps to monitor coastal lines has made utilizing multi-source remote sensing data and geographic information systems (GIS) extremely crucial.

All previous studies in the study area studied the changes that occurred in the shoreline over previous periods. However, in this study, I studied the effect of the protective means installed on the Rosetta Coast to protect hot areas from corrosion, how much protective measures help to lessen erosion along the Rosetta Coast, and how much of an impact the protective measures have on other portions of the coastline.

To safeguard the Rosetta promontory region, this study will monitor changes in the shoreline between 1980 and 2023, analyze the effects of erecting man-made wave barriers on the eastern and western sides, and gauge the rates of erosion and accretion. The study uses the DSAS tool in GIS to analyze the five Landsat satellite photos taken at different times (1980, 1990, 2000, 2010, 2023) to examine how the sedimentation and eroding patterns of the Rosetta coastline changed over time. The study area is characterized by the presence of coastal development such as the Ghalioun Sea hatchery. The research findings demonstrated that, despite the construction of artificial barriers in front of and on either side of the Rosetta Promontory, the topography of the region had altered considerably over the study period. Continuous monitoring of the shoreline in the Rosetta area is necessary to preserve the shoreline for sustainable development and coastal environment protection.

2. Protection Structures

To address the erosion issues, protective engineering features such as groins and revetments were built. Two seawalls, measuring 1.5 and 3.5 kilometers, were built inland at the western and eastern sides of Rosetta promontory, respectively, between 1986 and 1991 (see Figure 2) [24]. The seawall is 6.75 meters high and 48 to 70 meters wide, with an armor weight of 4 to 7 tons [25].

Marine protection of the western shoreline of Rosetta City. The project aims to protect the retreating shoreline of this area. The fact that the erosion rate has reached 50 m per year mandates the protection works in this region, which extend for a length of around 5 km. This area is also important due to its potential for investments in tourism. The project consists of constructing nine marine heads along the coastline of a length ranging between 250-450 m. These heads are located 650 m apart, and the scope of work involves using geotextiles, dolomite, and other materials in the protection works. The protection was completed in 2010 [26].

Between 2003 and 2005, five rubble mound groins, each measuring around 500 meters in length, with a 900-meter gap between them, were built inland to shield approximately 5 kilometers on the eastern side from severe erosion [27].

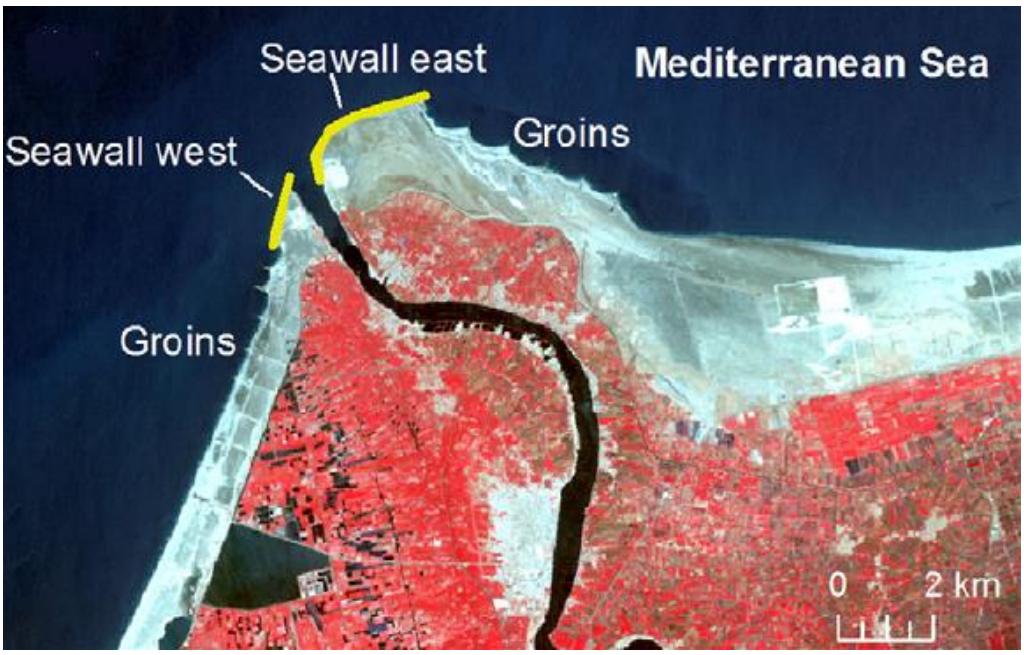

Figure 2. Illustrates the Construction of Seawalls and Groins at Rosetta Promontory [12]

Groins are constructed perpendicular to the coast. They directly impede longshore transit at the location, and they shield the surrounding region from wave action. The addition of an additional neighboring groin with the same length as the fifth groin and a separation of around 100 meters allowed the system's fifth groin to be transformed into an inlet, as seen in Figure 3. The Shore Protection Authority (SPA) built eight groins between the entrance and the exit, and the distance between the outlet and inlet was around 2.5 kilometers. The outflow aperture is around thirty meters wide. Additionally, eight groins were established by SPA and are located east of the outlet [10].

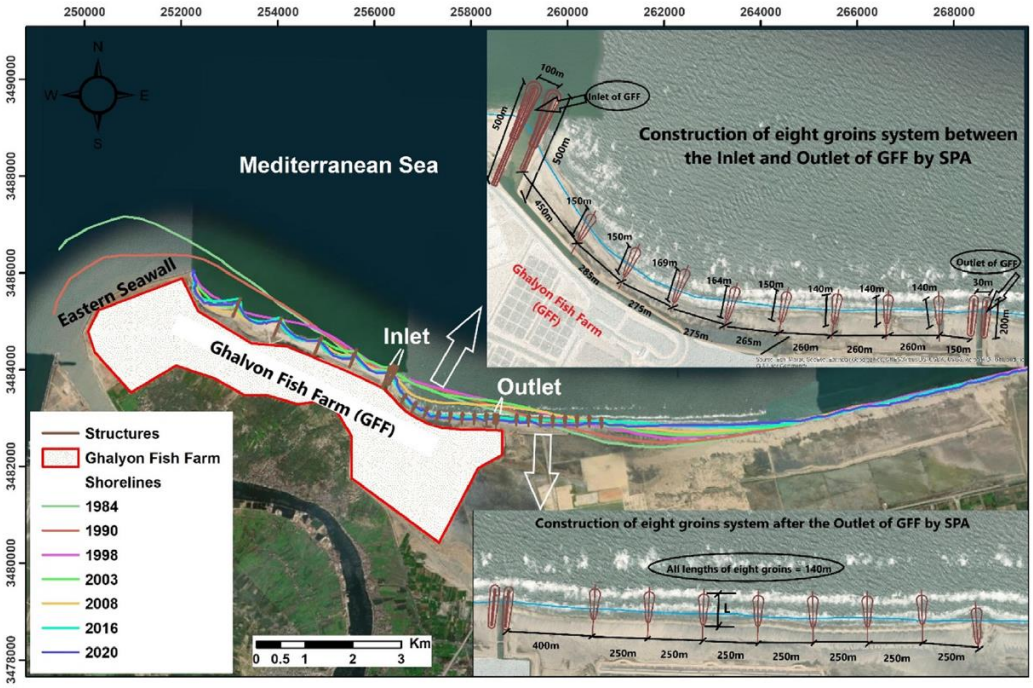

Figure 3. The Protective works of the Eastern shoreline of Rosetta [10]

3. Study Area

Many significant Egyptian cities, including Alexandria, Port Said, Rosetta, and Damietta, are located along the Mediterranean coast and might be impacted by Sea Level Rise (SLR) and climate change. One of the world's biggest deltas is the Nile Delta. It is situated where the Nile River splits and empties into the Mediterranean Sea in Northern Egypt Figure 4. The Delta coastline stretches 240 kilometers across the Mediterranean. The Delta has an area of over 22,000 km^2 [9].

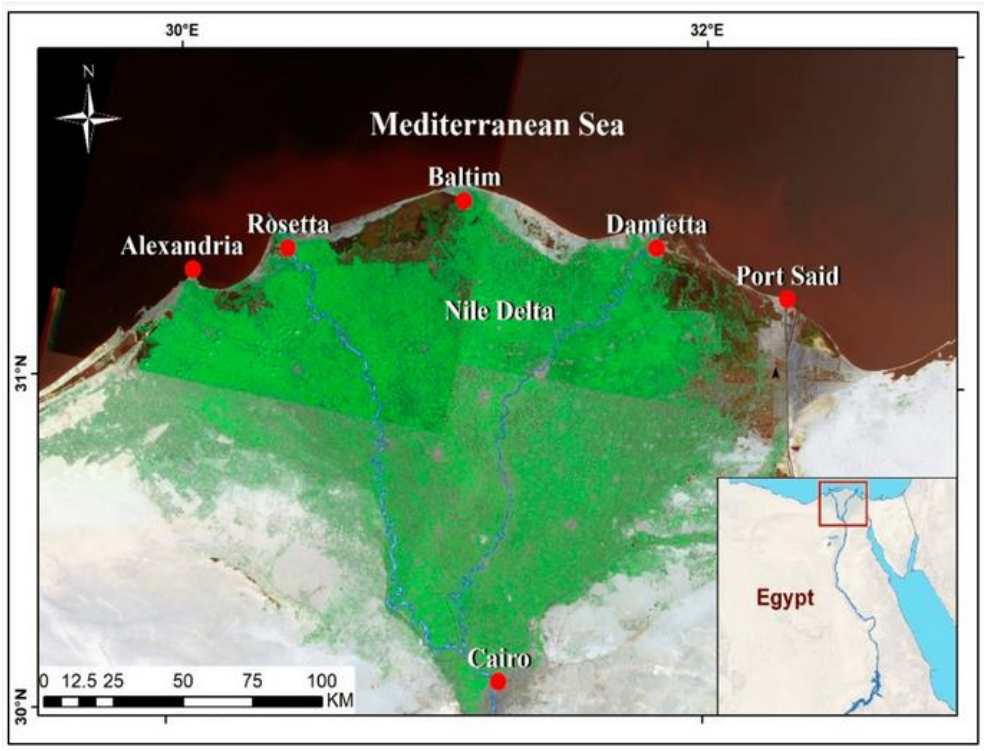

Figure 4. Location map of cities in the Nile Delta [9]

One of the coastal regions of the Nile Delta that is thought to be the most susceptible is Rosetta Promontory. As seen in Figure 5, it is located on the northwest shore of the Nile Delta. Due to its importance in transportation, agriculture, and fishing, this promontory is among the most significant locations. The promontory is a seaside headland with flat terrain covered with tiny sand dunes and sand mounds. The fine to extremely fine quartz sand that makes up the beach is abundant in heavy minerals [22].

Figure 5. Location map of the Study Area for Rosetta Promontory (Explore Google Earth, 2024) [28]

4. Data Set and Methodology

- To track shoreline changes, this study employed Landsat multitemporal satellite imagery. The satellite types and acquisition times, as well as the imagery data used, are listed in Table 1. Landsat images for these different periods in the study area were downloaded from [29].
- The images in the study area are using the UTM coordinate system, zone 36 N.
- Radiometric calibration was done for these images, and then Flaash Atmospheric Correction was done for these images using ENVI 5.3 software.

Table 1. The satellite types and acquisition times used to obtain the shorelines in the study area

Date Acquired	Spacecraft ID	Sensor ID	Resolution (m)
09/10/1980	LANDSAT_2	MSS	60
15/05/1990	LANDSAT_4	TM	30
05/07/2000	LANDSAT_5	TM	30
18/08/2010	LANDSAT_5	TM	30
13/07/2023	LANDSAT_8	OLI_TIRS	30

- Shorelines are drawn for the five Landsat images for different periods by separating seawater from the shoreline by using a color slice.
- Exported the color slice for all periods to the shape files to be used in ArcGIS 10.4.
- Using the ArcGIS 10.4 software to convert the feature polygon of shorelines obtained from ENVI 5.3 to the feature line.
- Downloading the DSAS V5 tool from https://code.usgs.gov/cch/dsas [30].
- Created a personal geodatabase and put within it a feature class for coastlines and baselines.
- Establishing a baseline to start making transects, as it is 300 meters away from the oldest shoreline, which is (1980).
- From the DSAS tool, data is entered that is used to perform statistical analysis of the layers of shorelines and the baseline. The distance between transects was set at 100 m.
- Calculate the evaluation elements SCE, NSM, EPR, and LRR for all sectors from the Calculate rates in DSAS (see Figure 6).

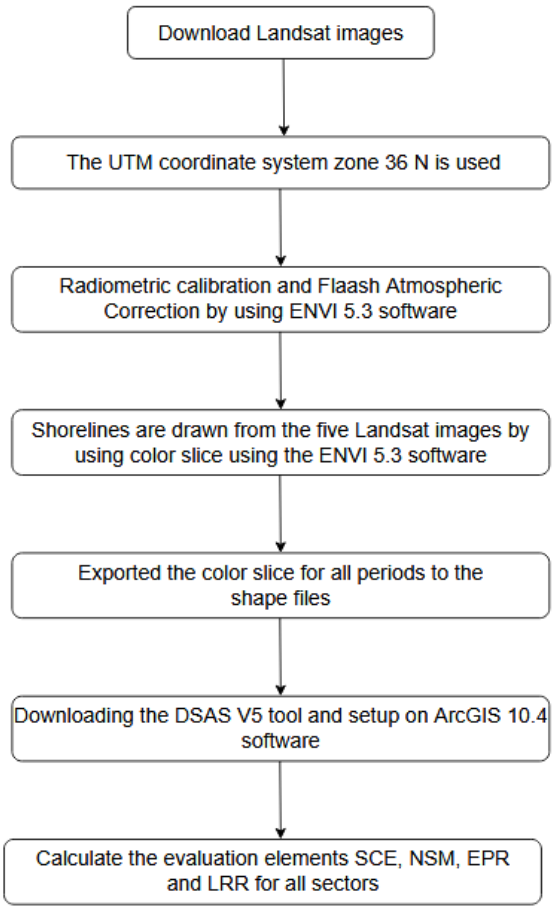

Figure 6. Block diagram that represents the steps used to Calculate the evaluation elements SCE, NSM, EPR and LRR

5. The Shoreline Changes Determination

The difference between the extracted and baseline shorelines is the conventional approach for computing the shoreline change statistics, and the U.S. Geological Survey developed the DSAS module as an add-on for the ArcGIS

program [31]. The difference between the coastline that was farthest from and closest to the baseline was used to compute the SCE [32], and the change rate in the shoreline was calculated using EPR and LRR. The overall positional movement of the shoreline within a particular period was determined using NSM [31]. The baseline, shorelines, and transect line are the three elements that are necessary to evaluate shoreline changes.

5.1. End Point Rate (EPR)

The distance of shoreline movement divided by the time interval between the oldest and most recent shoreline yields the end point rate [33]. Because it requires little in the way of shoreline data and is simple to compute, EPR is regarded as one of the finest methods for assessing shoreline change [34].

$$EPR = \frac{L_2 - L_1}{t_2 - t_1} \quad (1)$$

where t_1 and t_2 are the time intervals between the most recent year and the furthest year; L_1 and L_2 are the lengths, respectively, between the shorelines in the most recent year and the farthest year to the baseline (see Figure 7) [35].

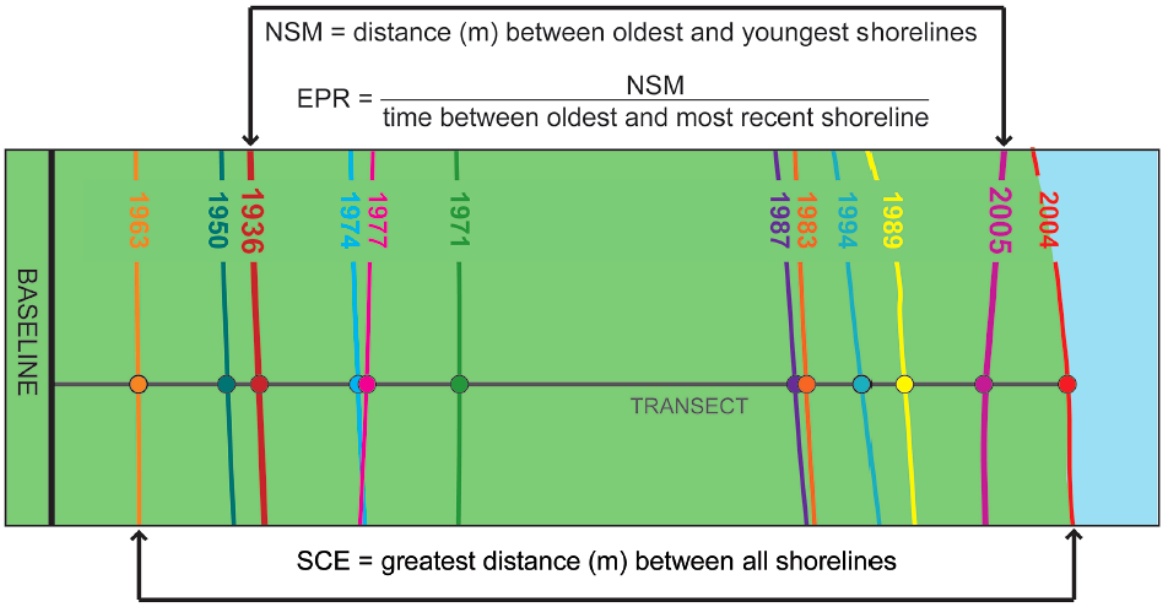

Figure 7. Represent how the values of EPR, NSM and SCE are computed [36]

5.2. Net Shoreline Movement (NSM)

For each transect, the NSM is computed as the difference between the oldest and youngest shoreline, expressed in meters, see Figure 7. Equation 2 is used to determine the NSM of a transect in this investigation [37].

NSM= Distance (Oldest shoreline – Young shoreline) (2)

5.3. Shoreline Change Envelope (SCE)

The shoreline change envelope (SCE) reports a length (m) instead of a rate. The SCE value (see Figure 7) represents the longest distance among all coastlines that intersect a given section. The results of SCE stay positive since there is no sign in the total length among both coastlines [36, 37].

$$SCE = \text{Distance}(\text{Shoreline}_{\text{Farthest}} - \text{Shoreline}_{\text{Nearest}}) \quad (3)$$

5.4. Linear Regression Rate (LRR)

Fitting a least-squares regression line to every coastline point for a transect yields a linear regression rate-of-change statistic (see Figure 8). The regression line is positioned to minimize the total of the squared residuals, which are calculated by squaring each data point's offset distance from the regression line and adding the squared residuals together. The slope of the line represents the linear regression rate [36].

Below is the linear regression equation (Equation 4) [38] that is used to determine the coastline movement:

$$L = b + mx \quad (4)$$

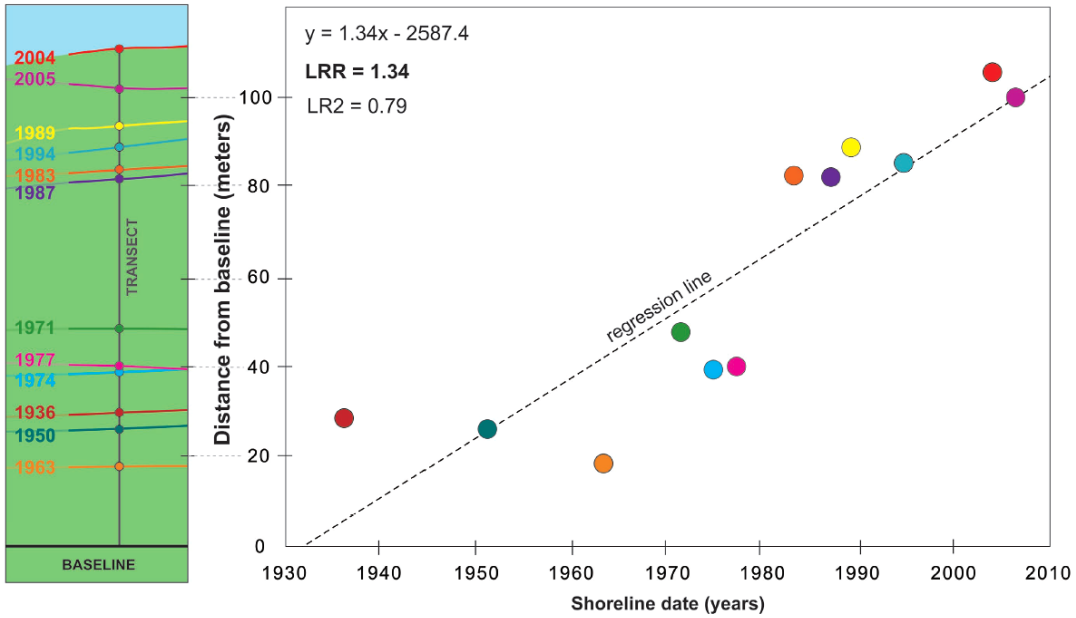

Figure 8. Represent how the value of Linear Regression Rate (LRR) is computed [36]

6. Results

In this research, to extract the shoreline of the Rosetta Promontory from the five Landsat images of the study area, we used the ENVI software by using the color slice to distinguish between the shoreline and the water in all the Landsat images used. In Figure 9, the shoreline was extracted from the Landsat image in 1980 and appears in yellow. The shoreline in 1990 was extracted from the Landsat image, where the shoreline appeared in cyan in Figure 10. The shoreline was extracted from the Landsat image in 2000 and appears purple in Figure 11. The same tool was used to extract a shoreline from a Landsat image in 2010, which appeared in blue (see Figure 12). Finally, the shoreline was extracted in 2023 from the Landsat image and appeared in red (see Figure 13). Also, Figure 14 shows the differences between the locations of the shorelines of the Rosetta region for the periods from 1980 to 2023. This shows the effects on the shoreline over the period of the study.

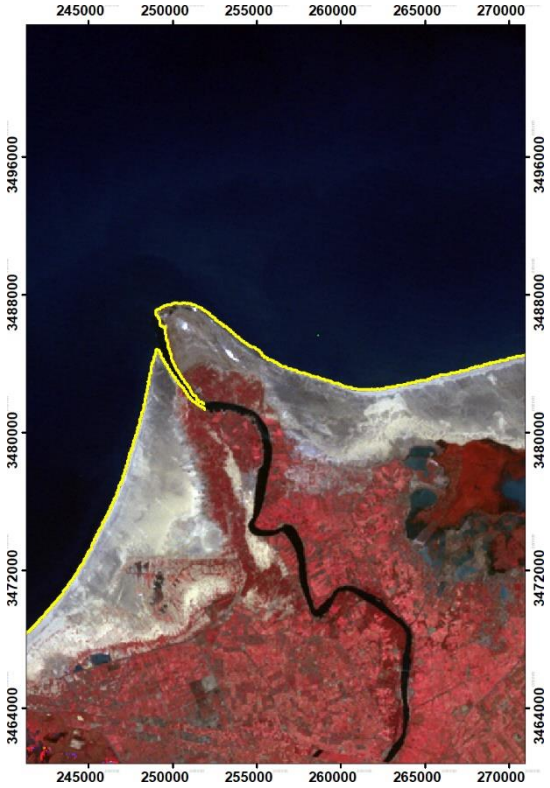

Figure 9. The shoreline of the Rosetta Promontory for the period 1980

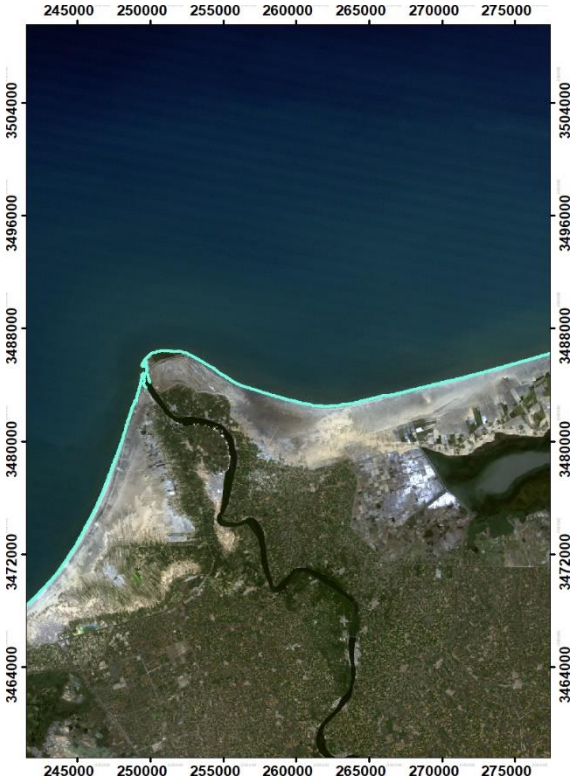

Figure 10. The shoreline of the Rosetta Promontory for the period 1990

Figure 11. The shoreline of the Rosetta Promontory for the period 2000

Figure 12. The shoreline of the Rosetta Promontory for the period 2010

Figure 13. The shoreline of the Rosetta Promontory for the period 2023

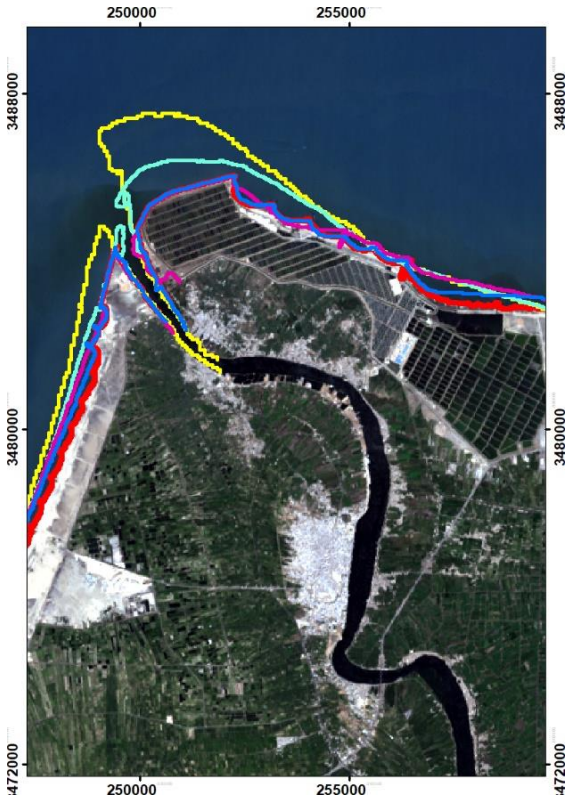

Figure 14. The shoreline of the Rosetta Promontory the period 1980 –2023

After the shapefiles were opened on the GIS software, it converted the feature polygon to the feature line to make a merge of parts for each shoreline of the five shorelines. The DASA tool is then used to perform a statistical analysis of these shorelines.

Figures 15 to 17 show the statistical analysis between each of the two successive periods using the DSAS tool by calculating NSM, EPR, and SCE. It became clear to us from Figure 15 that the highest erosion on the Rosetta shoreline, especially at Rosetta Promontory, occurred in the period from 1980 to 1990. In the period 1990–2000, the erosion occurred on the Rosetta Promontory and extended east near the Ghalioun Sea hatchery and westward to the vicinity of Rosetta Tongue. This erosion is severe and noticeable, as is evident from Figure 14, where the yellow color represents the shoreline in 1980, the cyan color represents the shoreline in 1990, and the purple color shows the shoreline in 2000. Figure 15 illustrates that the NSM is higher in the periods (1980–1990) and (1990–2000) in transects from 210 to 270, and thus these transects have the highest rate of erosion. Also in this period, the same transects in Figure 16, which represents the EPR value, gave the highest values, and these transects also gave the highest values in the SEC (see Figure 17). In the period 1980–1990, the maximum erosion rate was about 140 m/year at the Rosetta Promontory. In the period from 1990 to 2000, the maximum erosion of the shoreline was about 101.71 m/year at the Rosetta Promontory.

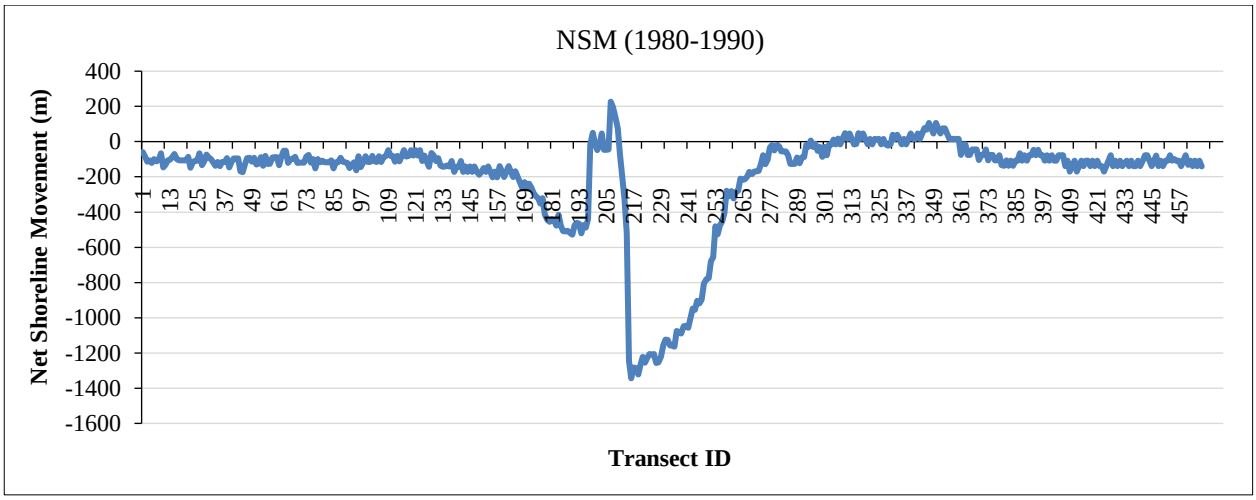

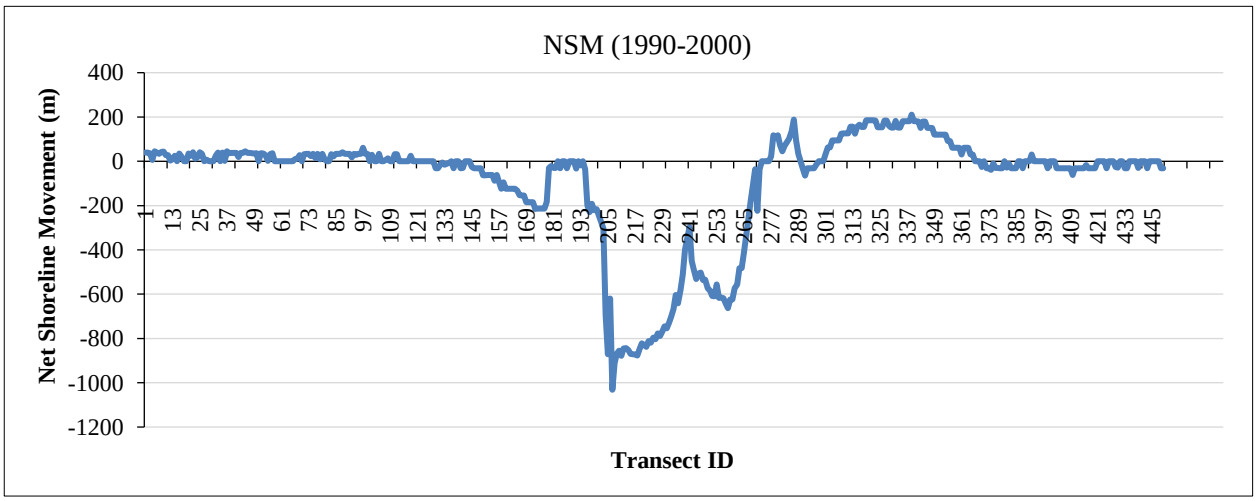

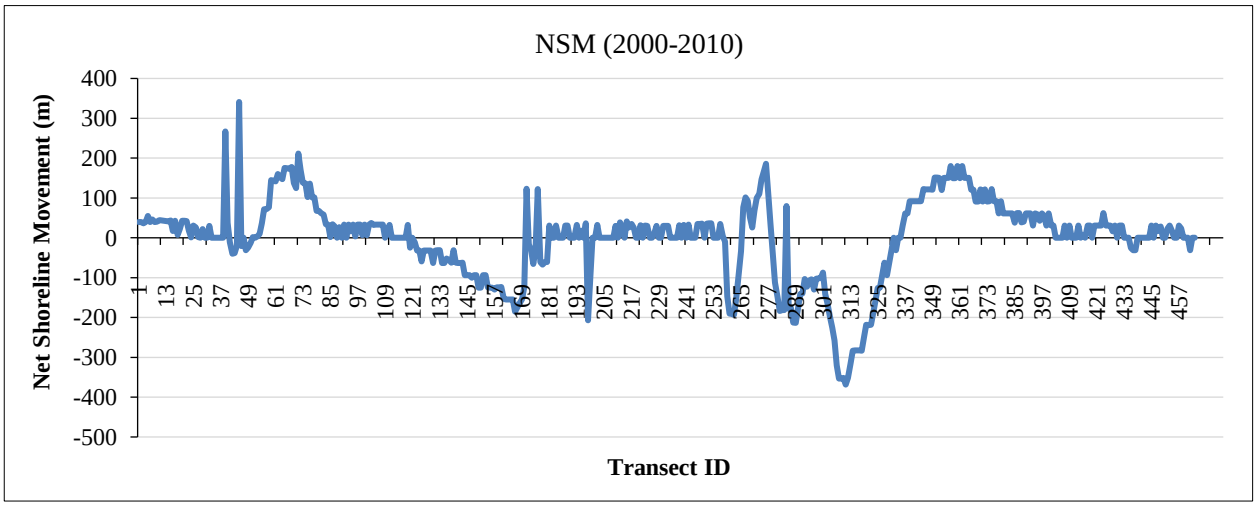

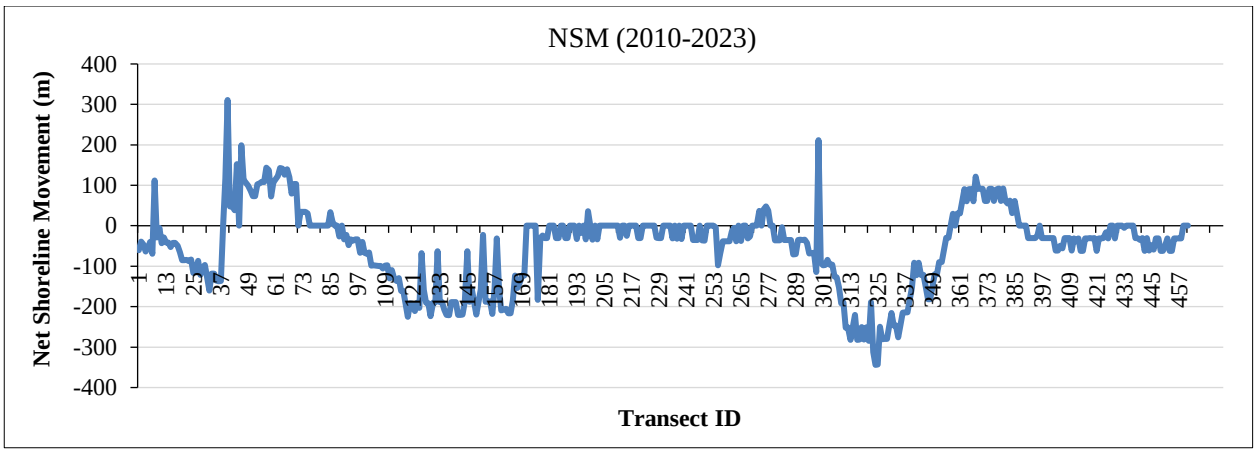

Figure 15. The statistical outcomes for NSM over a variety of historical intervals (1980-1990)- (1990- 2000)- (2000–2010)- (2010–2023)

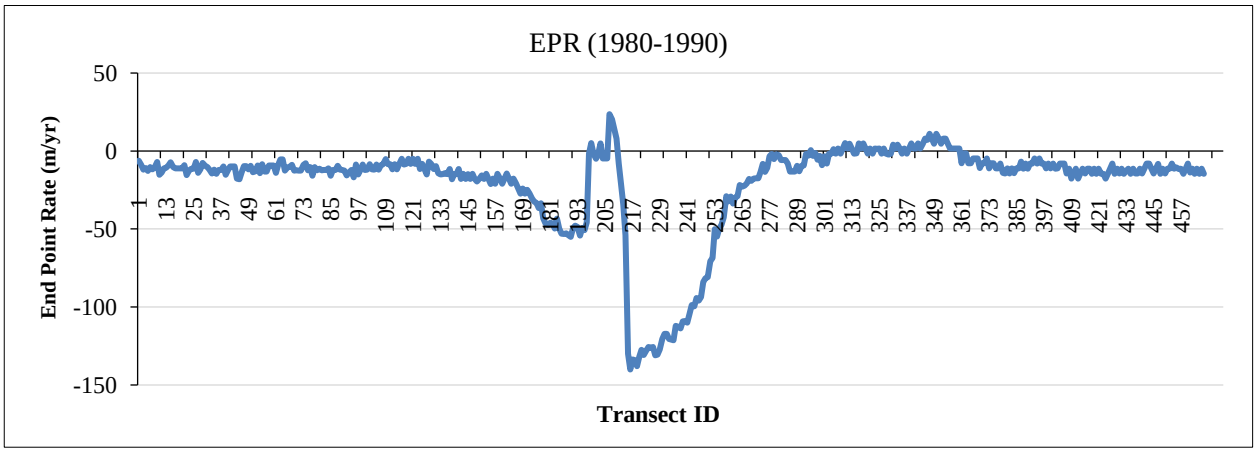

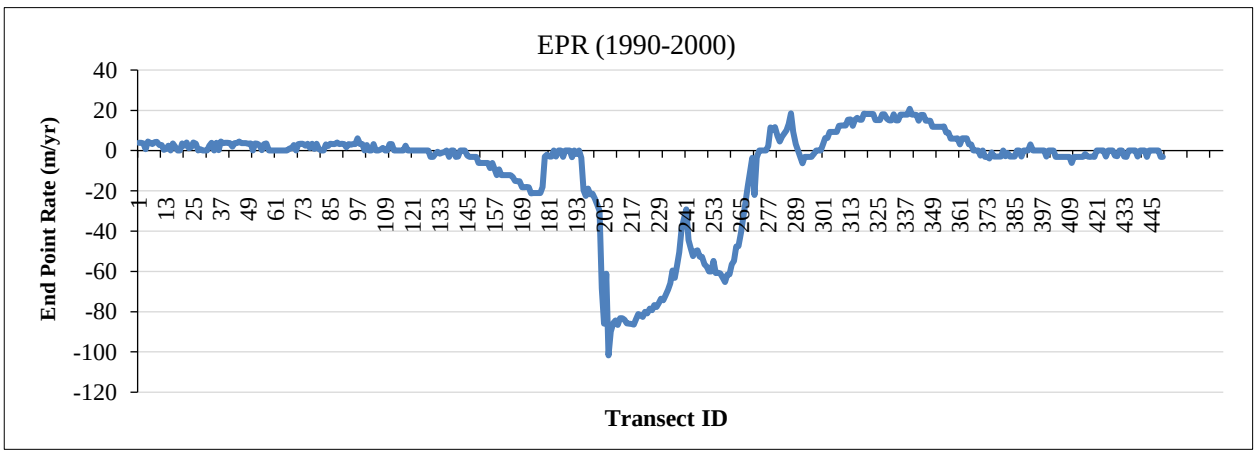

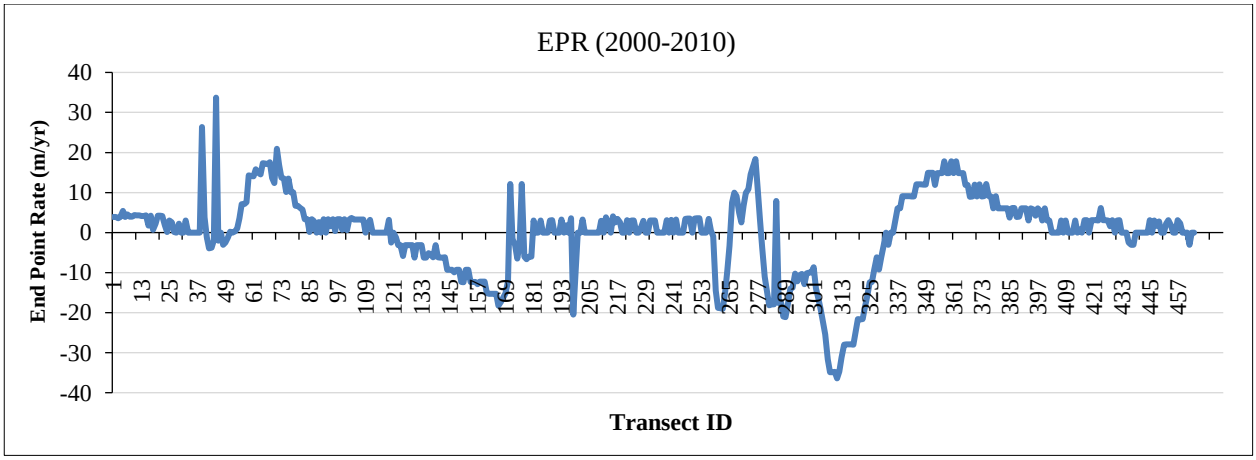

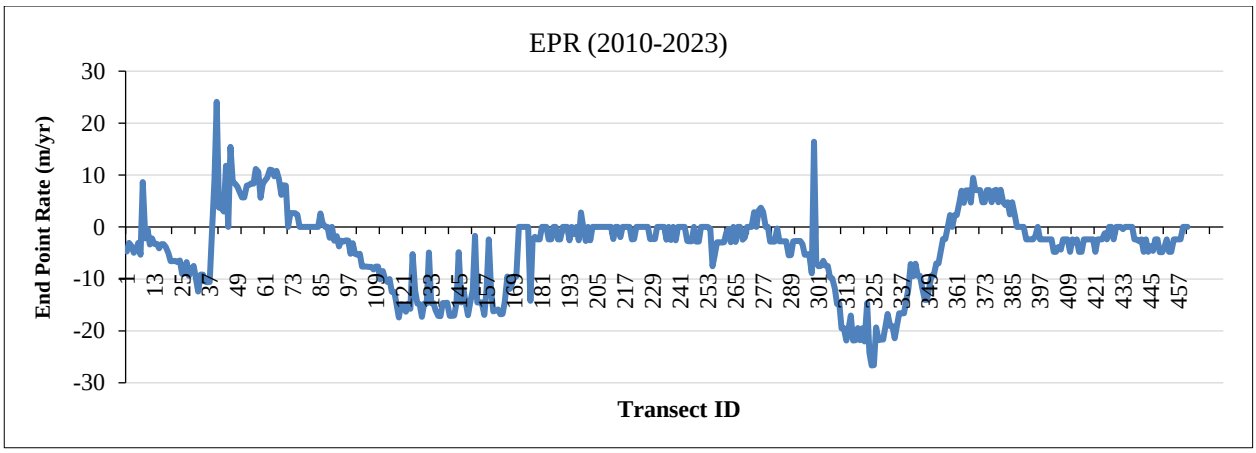

Figure 16. The statistical outcomes for EPR over a variety of historical intervals (1980-1990)- (1990–2000)- (2000–2010)- (2010–2023)

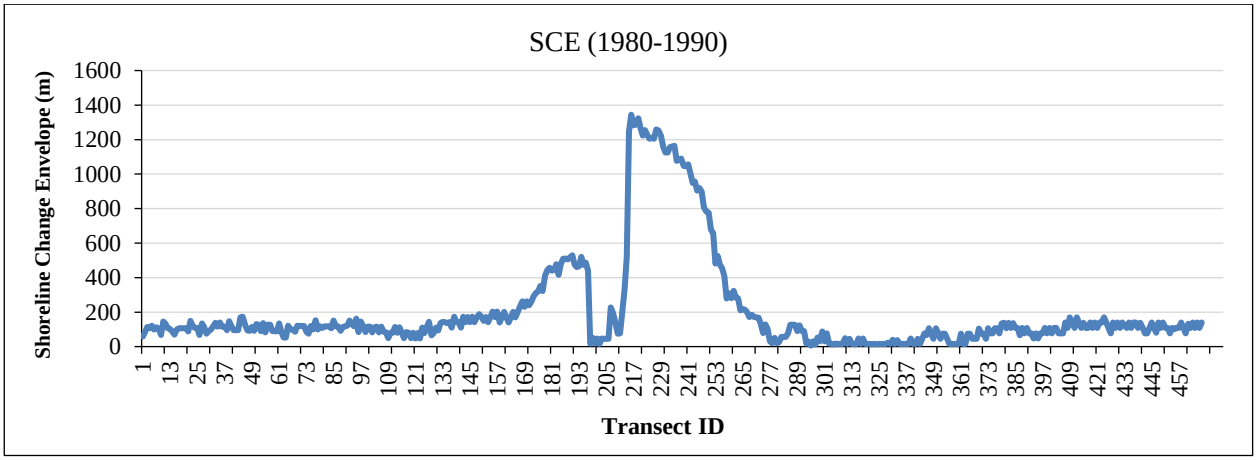

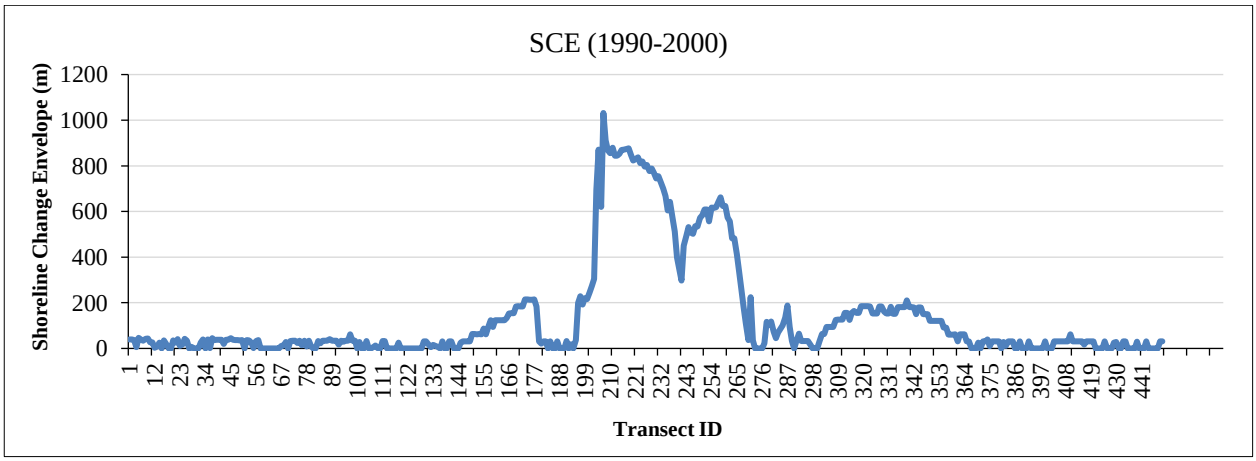

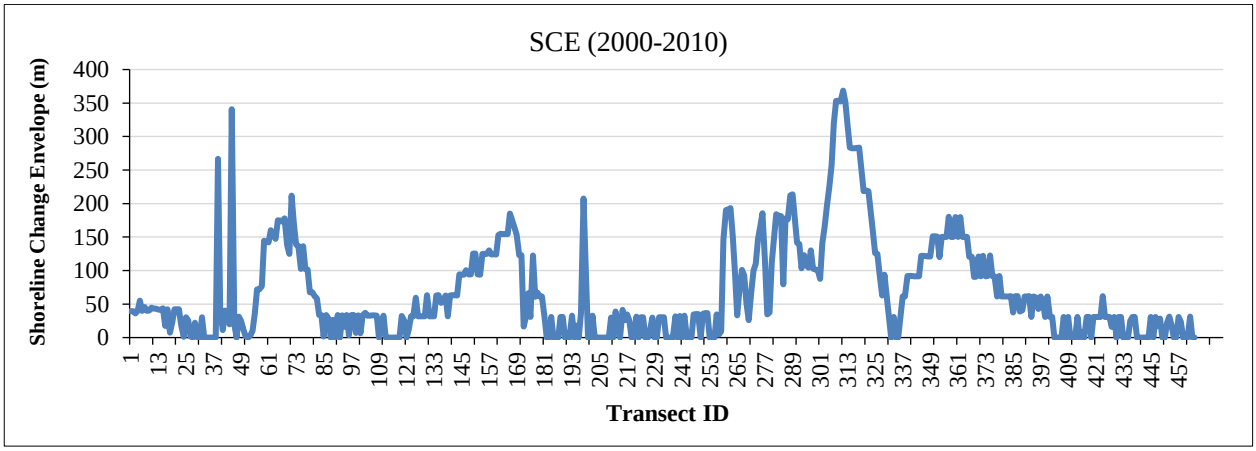

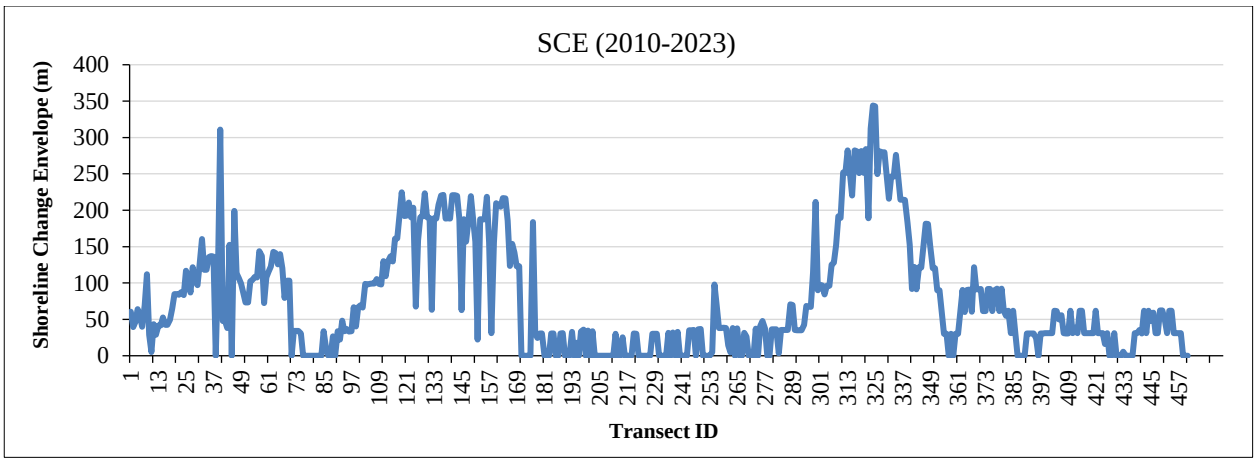

Figure 17. The statistical outcomes for SCE over a variety of historical intervals (1980-1990)- (1990–2000)- (2000–2010)- (2010–2023)

In the period between 1991, two Seawalls were built, one on the western side of the Rosetta Promontory and the other on the eastern side of the estuary, to confront erosion operations. This addressed the problem of erosion on the eastern and western sides near the Rosetta Promontory or in the protection area, but over the years, erosion occurred in the eastern and western regions. After the protection walls, this is evident in Figure 15.

In the period (2000-2010) and the period (2010-2023) occurred in which the shoreline remained largely stable in the area of the protection walls that were established on the eastern and western sides of the Rosetta Promontory this appears in the shoreline 2000, 2010, and 2023 (see Figure 15), but there was a change in the shoreline in the areas after the protection walls in the eastern and western regions, as in Figure (15), where the change occurring in the eastern region increased with the progress the time, and this is evident in transect 287 to transect 330 in the period (2000-2010), then there was an increase in the number of transect in the period (2010-2023), that from sector 280 to 351.

Also, erosion occurred in the western region of Rosetta Promontory after the protection walls; the erosion increased with progressive time, as this appears in transects 120 to 165 during the period (2000-2010). Then there was an increase in the number of erosions transects from 100 to 170, and then from transect 11 to transect 40 in the period (2010-2023) (see Figure 15). Additionally, the shoreline changes on the eastern and western sides behind the protection of Rosetta Promontory in the same periods in the EPR values (see Figure 16) and in the SCE values (see Figure 17). In the period between 2000 and 2010, there was a decrease in erosion, as the maximum erosion reached about 36.42 m/year. Also, in the period from 2010 to 2023, the erosion decreased, and the maximum erosion reached about 26.66 m/year.

Figures 18 to 21 show that the change in the shoreline from one period of time to another is not only erosion but also accretion. The area of erosion and accretion between the Rosetta shorelines in 1980 and 1990 was calculated to be about 8.35 km^2 and 0.36 km^2, respectively. The area of erosion and accretion between the years 1990 and 2000 was approximately 4.12 km^2 and 1.29 km^2, respectively.

The area of erosion and accretion between the years 2000 and 2010 was 1.72 km^2 and 1.50 km^2, respectively. Finally, the area of erosion and accretion between the years 2010 and 2023 was approximately 3.03. km^2 and 0.62 km^2, respectively. Table 2 shows the maximum, average, and minimum values of EPR, NSM, and SCE for the Rosetta shoreline at several periods (1980-1990), (1990-2000), (2000-2010), and (2010-2023).

Table 2. The statistical outcomes for EPR (m/yr.), NSM (m) and SCE (m) in time intervals (1980-1990)- (2000–2010)- (1990–2000)- (2010–2023)

Historical Intervals	Subject	EPR (m/yr)	NSM (m)	SCE (m)
1980 to 1990	Maximum	23.62	226.58	1343.93
	Mean	-20.42	-195.96	205.82
	Minimum	-140.07	-1343.93	5.31
1990 to 2000	Maximum	20.76	210.55	1031.60
	Mean	-8.51	-86.29	141.46
	Minimum	-101.71	-1031.6	0
2000 to 2010	Maximum	33.7	340.94	368.5
	Mean	-0.14	-1.41	68.66
	Minimum	-36.42	-368.5	0
2010 to 2023	Maximum	24.1	310.9	343.94
	Mean	-3.98	-51.36	78.19
	Minimum	-26.66	-343.94	0

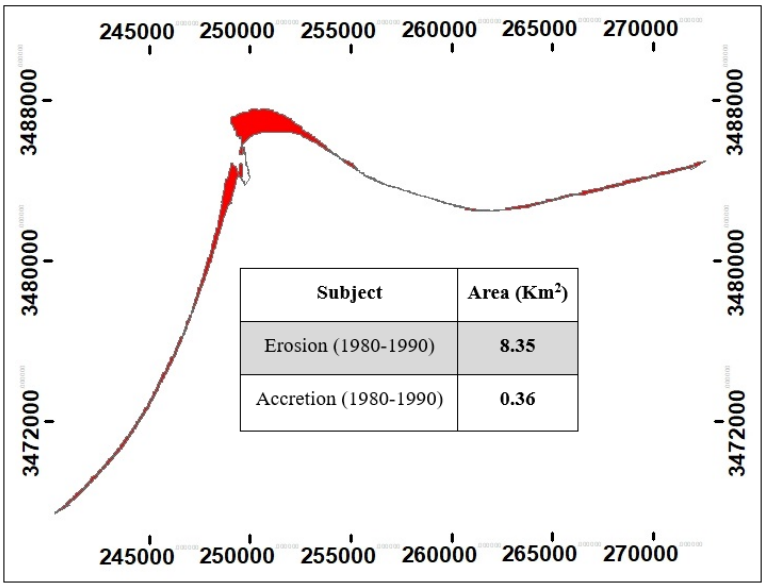

Figure 18. The computation of erosion and accretion areas in the shoreline of the Rosetta Promontory in 1980 and 1990

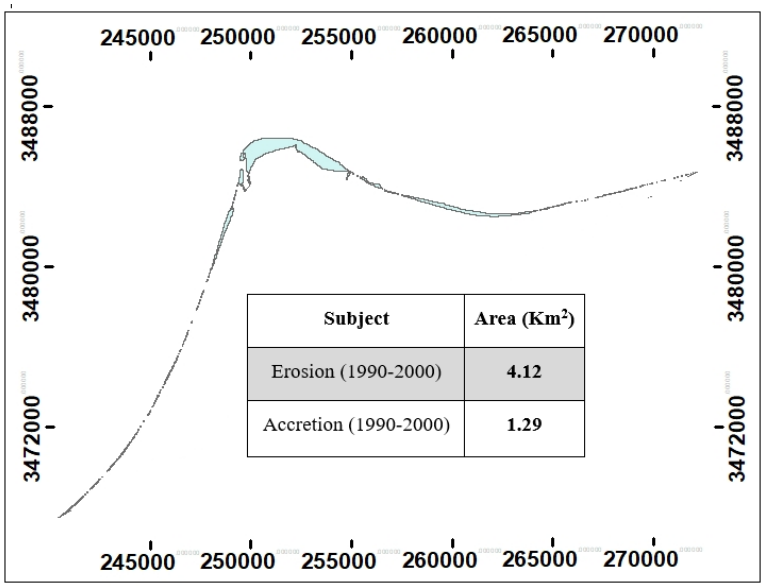

Figure 19. The computation of erosion and accretion areas in the shoreline of the Rosetta Promontory in 1990 and 2000

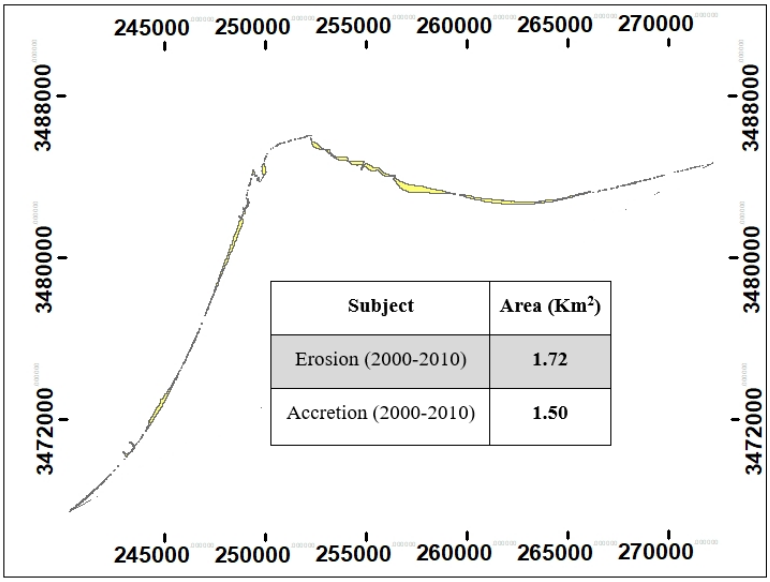

Figure 20. The computation of erosion and accretion areas in the shoreline of the Rosetta Promontory in 2000 and 2010

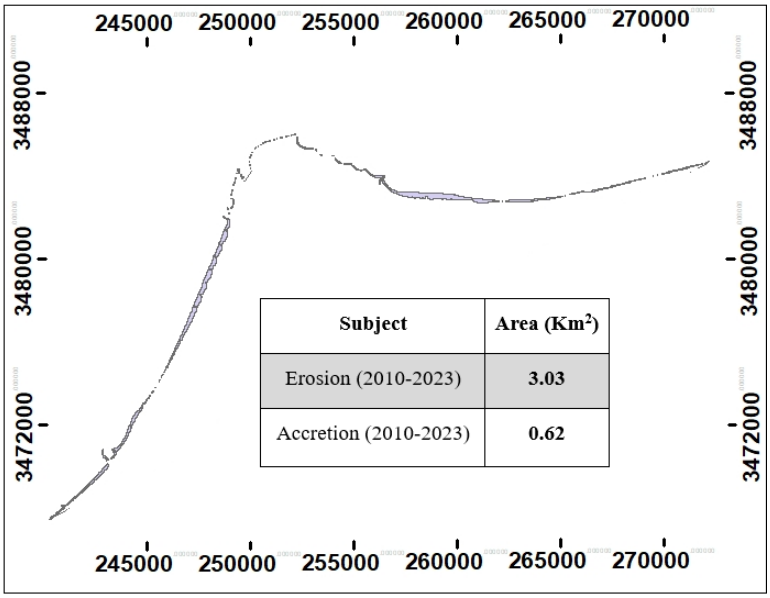

Figure 21. The computation of erosion and accretion areas in the shoreline of the Rosetta Promontory in 2010 and 2023

The present study involved the extraction of the Rosetta shoreline from multitemporal Landsat satellite photos covering the following years: 1980, 1990, 2000, 2010, and 2023. For over 43 years, the ArcGIS software DSAS tool was used to track changes in the Rosetta shoreline. To account for changes in the shoreline, a baseline was established 300 meters from the old Rasheed Promontory shoreline in the year 1980 and parallel to this shoreline towards the sea. A total of 1583 transects with a length of almost 160 kilometers were formed, with a 100-meter space between each two transects respectively. The results of statistical methods SCE, EPR, NSM and LRR calculated by DSAS are summarised in Table 3. The maximum erosion rate from 1980 to 2023 was about 50.14 m/year.

Table 3. The statistical outcomes for EPR (m/yr), NSM (m), SCE (m) and LRR (m/yr) between 1980 and 2023

Time Interval	Subject	EPR (m/yr)	NSM (m)	LRR (m/yr)	SCE (m)
1980-2023	Maximum	8.55	365.64	9.05	2143.95
	Mean	- 3.51	-150.06	-2.96	251.02
	Minimum	-50.14	- 2143.95	- 47	18.64

Figures 22 to 25 represent the statistical analysis of EPR, NSM, SCE, and LRR for several periods' times of the Rosetta shoreline in 1908, 1990, 2000, 2010, and 2023. Where these shorelines merged and calculated the values of EPR, NSM, SCE and LRR for the Rosetta shoreline at 1583 transects over 43 years.

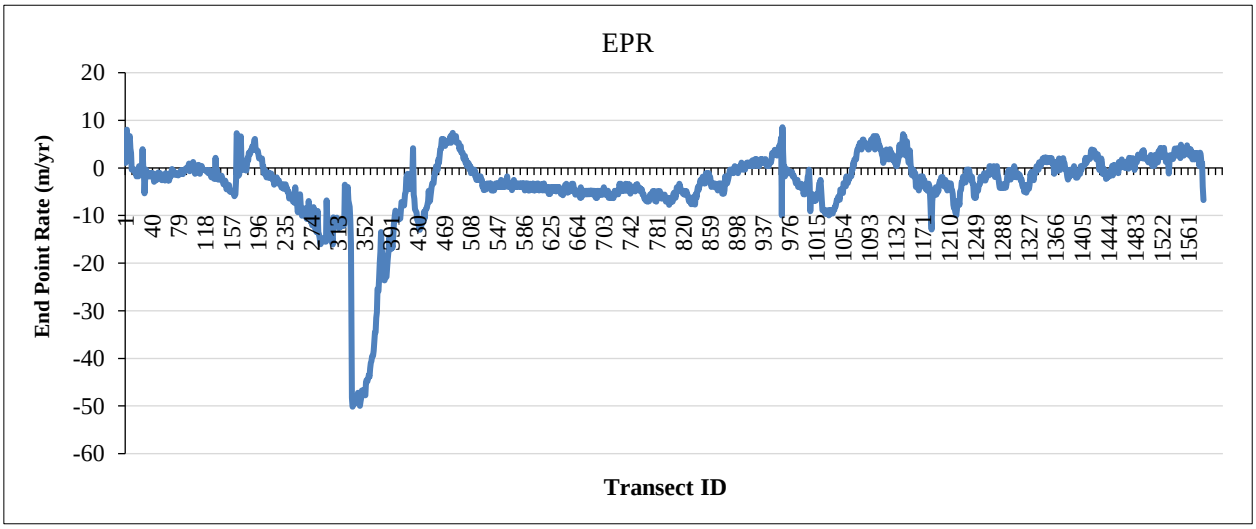

Figure 22. The statistical outcomes for EPR between 1980 and 2023

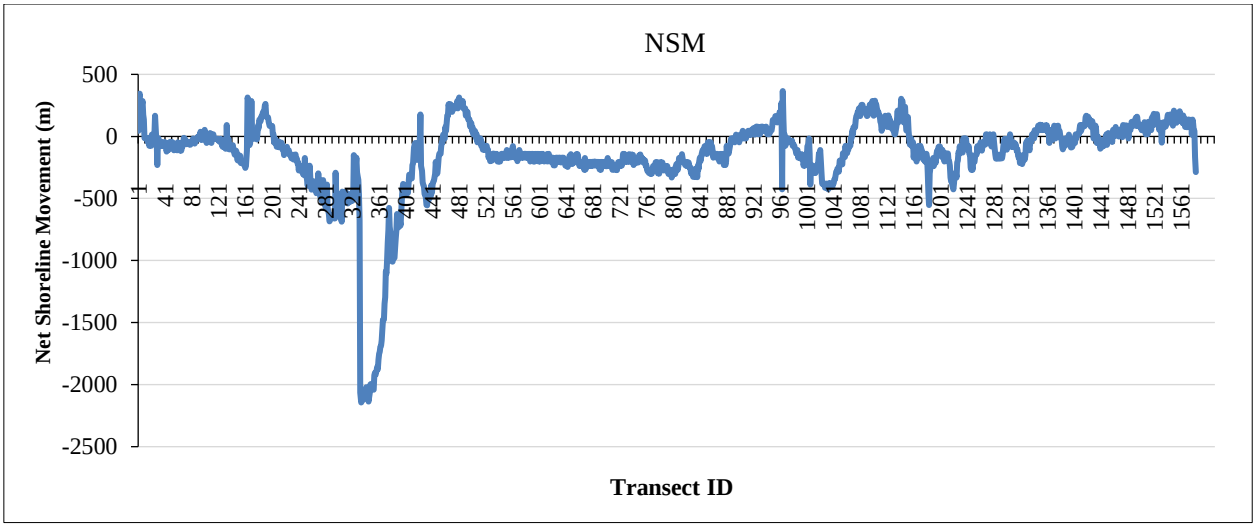

Figure 23. The statistical outcomes for NSM between 1980 and 2023

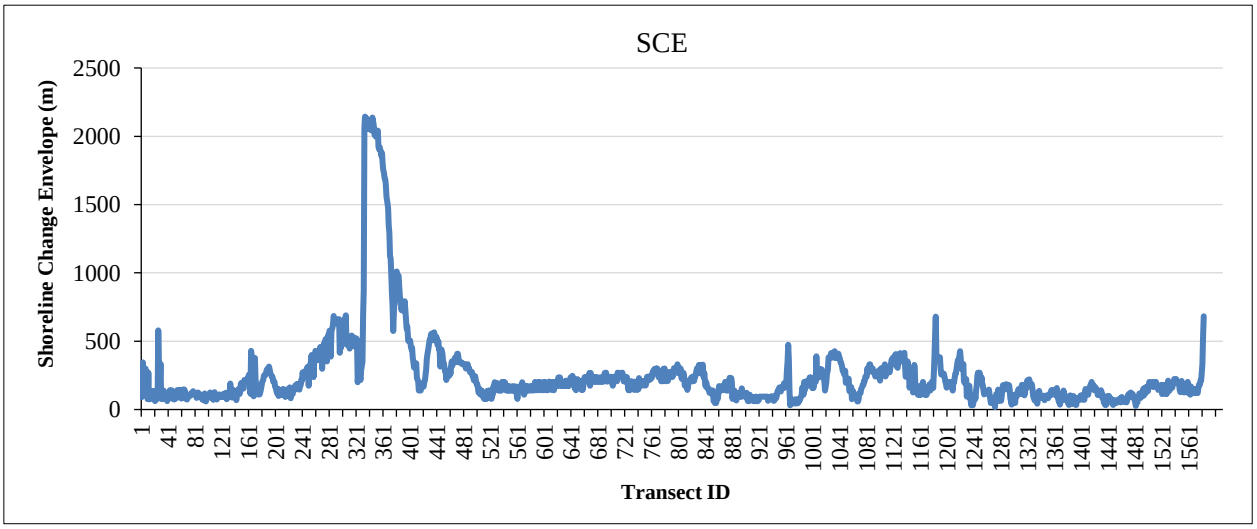

Figure 24. The statistical outcomes for SCE between 1980 and 2023

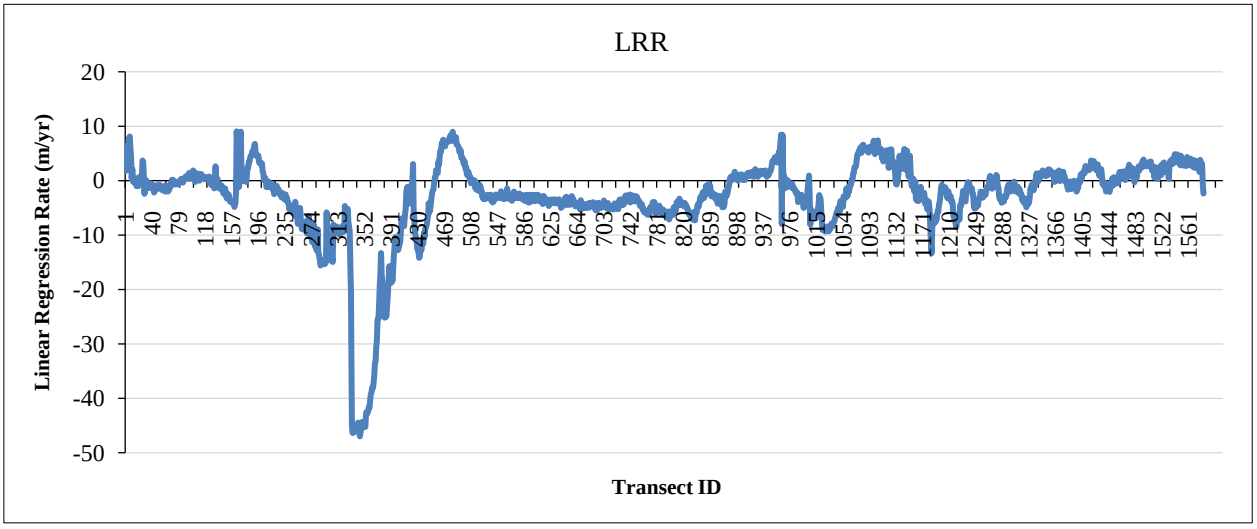

Figure 25. The statistical outcomes for LRR between 1980 and 2023

7. Discussion

Based on previous studies of the Rosetta shoreline over different periods, it is clear to us that there is erosion occurring on the Rosetta shoreline, but the rate of erosion per year varies from one study to another. These results depend on the duration of the period during which the erosion statistics are calculated (see Table 4).

Table 4. Summarizes the Previous Studies to determine the erosion rate of Rosetta Shoreline

Previous Studies	Period Time	Erosion rate
Ghoneim et al. (2015) [12]	1991 to 2012	Maximum rate 30 m/year
Masria et al. (2015) [20]	1984 - 2014	Maximum rate 37 m/year
Deabes (2017) [21]	1970 to 2010	Average rate 60 m/year
Balbaa et al. (2020) [11]	1985 to 1990	Maximum rate 37 m/year
	1985 to 2015	Maximum rate 50 m/year
Fouad et al.2020 [22]	1984 to 1995	Maximum rate 127 m/year
	1995 to 2004	Maximum rate 45 m/year
	2004 to 2011	Maximum rate 45 m/year
	2011 to 2019	Maximum rate 59 m/year

The results of this research study to calculate the erosion of the Rosetta shoreline for each year were calculated over about 43 years. The erosion was also calculated for four time periods, each period representing about 10 years. In each period, the means of protection were studied and the extent of their impact on reducing the rate of erosion. The following is a summary of the protection means in the periods of the study and the extent of their contribution to reducing annual erosion:

- The Rosetta shoreline from 1980 to 1990, recorded the maximum erosion rate, which was about 140 m/year, at the Rosetta Promontory.
- The erosion rate was reduced in the Rosetta shoreline in the period from 1990 to 2000, the maximum erosion of the shoreline was about 101.71 m/year at the Rosetta Promontory, because of the work of two seawalls on the eastern side and the western side of Rosetta Promontory in the period from 1986 and was completed in 1991.
- During the period between 2000 and 2010, there was a decrease in erosion, as the maximum erosion reached about 36.42 m/year due to two seawalls and also due to the construction of many groins on the eastern and western sides after the walls established at the Rosetta Promontory, where five hills of rubble were created east of the protection wall between 2003 and 2005 and nine vertical heads were also constructed on the west after the protection wall, and they were completed in 2010.
- In the period from 2010 to 2023, the maximum erosion reached about 26.66 m/year, as the Shore Protection Authority established 16 groins on the eastern side of Rosetta Promontory, which were recently completed.
- The study showed that the maximum erosion rate from 1980 to 2023 was about 50.14 m/year.

8. Conclusions

This research aims to look at one of the shorelines of the Delta in Egypt, which is the shoreline of the city of Rosetta. Due to the environmental changes that occur, which lead to the shorelines being affected by these changes, the delta area is one of the areas vulnerable to drowning because of the rise in the water level of the Mediterranean Sea. In this research, the area of the Rosetta Promontory of the Nile River and the eastern and western regions of this Rosetta Promontory were studied for approximately 43 years from 1980 to 2023. The shoreline was drawn over five time periods (1980 - 1990 - 2000 - 2020 - 2023). The following became clear to us:

- The impact of erosion was significant in the period between 1980 and 1990 in Rosetta Promontory and the eastern and western parts next to the Rosetta Promontory, where the area was about 8.35 km^2 and accretion was very small. Therefore, engineering structures were constructed between 1986 and 1991 to reduce erosion problems. Two barriers were built, one on the western side and the other on the eastern side of the Rosetta Promontory.
- In the period between 1990 and 2000, the area of erosion was less than the previous period, and the area of accretion increased, and this is due to the construction of protection seawalls.
- The protection seawalls led to no erosion at the Rosetta Promontory, but it appeared in the eastern and western regions that are away from the protection seawalls at the Rosetta Promontory, which led to an increase in the area of erosion in these areas during the period of the year From 2000 to 2010, although the Shore Protection Authority built groins system to protect the shorelines from erosion on the eastern and western sides. After the seawalls were established on the Rosetta Promontory on both sides, five hills of rubble, each about 500 meters long, were created on the eastern side between the years 2003 and 2005, and the construction of nine vertical heads on the Rosetta shoreline to protect 5 km west of the western seawall of the Rosetta Promontory. The length of each vertical head ranges between 250-450 meters and it was completed in 2010.
- In the period between 2010 and 2023, there was no erosion in the shoreline at the seawalls at the Rosetta Promontory, but the erosion increased in the eastern and western regions that are far from the protection seawalls.

- In the period from 2000 to 2010, the area of erosion during this period was about 1.72 km^2, and in the period from 2010 to 2023, it was about 3.03 km^2.
- Recently the sixteen groins were constructed by the Shore Protection Authority (SPA) on the eastern side of the five groins which were constructed between 2003 and 2005 on the eastern side after the East seawall of the Rosetta Promontory, this is to reduce the erosion at the eastern areas of the Rosetta Promontory.
- Although artificial barriers have been created on the eastern and western sides of the Rosetta Promontory, there is erosion in the shoreline between these artificial barriers, and therefore the regions of the eastern and western along the shoreline after Promontory Rosetta must be continuously monitored. In addition, monitor the existing various protection facilities and develop protection plans, if necessary to avoid increasing the area of erosion.

8.1. Recommendations

Because of the environmental and climatic changes along the shoreline, it is crucial to monitor erosion and buildup in places that are vulnerable to flooding. The study's findings suggest that erosion and accumulation change with time, according to this research I've done or the other studies for the which applied same study area. The shoreline alterations across several periods were analyzed in this research using satellite imagery. The delta is one of the hottest places on Earth as a result of environmental and climatic changes, and it will likely be flooded in the next several decades. As a result, various ideas and suggestions for monitoring coasts have been established; these can be summed up as follows:

- A variety of data collection methods, including high-resolution satellite imagery, aerial photos, images from drones, and ground surveying instruments like GPS and Total Station, are utilized to analyze shorelines. Ideally, the instruments used for ground surveying should be used to gather data.
- The coastline in the delta region, one of the most affected places, is monitored annually using one of the aforementioned techniques. In addition, extra monitoring is carried out in case any environmental phenomena occur.
- Geographic Information Systems (GIS) software is used to analyse the data and produce maps allowing to detection of erosion and accumulation.
- Delivering data, analysis, graphs, and suggestions to decision-makers regularly.
- Integration and coordination among organizations and bodies concerned with tracking rates of erosion and accumulation, assessing the development of coastal areas, keeping an eye on shifts in the vegetation cover, and researching the consequences of sea level rise to periodically monitor coastlines and report on them.

9. Declarations

9.1. Data Availability Statement

The data presented in this study are available in the article.

9.2. Funding

This study is supported via funding from Prince Sattam Bin Abdulaziz University project number (PSAU/2024/R/1445).

9.3. Conflicts of Interest

The author declares no conflict of interest.

10. References

[1] Chettiyam Thodi, M. F., Gopinath, G., Surendran, U. P., Prem, P., Al-Ansari, N., & Mattar, M. A. (2023). Using RS and GIS Techniques to Assess and Monitor Coastal Changes of Coastal Islands in the Marine Environment of a Humid Tropical Region. Water (Switzerland), 15(21), 3819. doi:10.3390/w15213819.

[2] Maiti, S., & Bhattacharya, A. K. (2009). Shoreline change analysis and its application to prediction: A remote sensing and statistics-based approach. Marine Geology, 257(1–4), 11–23. doi:10.1016/j.margeo.2008.10.006.

[3] Guariglia, A., Buonamassa, A., Losurdo, A., Saladino, R., Trivigno, M. L., Zaccagnino, A., & Colangelo, A. (2006). A multisource approach for coastline mapping and identification of shoreline changes. Annals of Geophysics, 49(1), 295–304. doi:10.4401/ag-3155.

[4] Aryastana, P., Ardantha, I., Eka Nugraha, A., & Windy Candrayana, K. (2017). Coastline changes analysis in Buleleng regency by using satellite data. The 1st Warmadewa University International Conference on Architecture and Civil Engineering, 20 October, 2017, Warmadewa University, Kota Denpasar, Indonesia.

[5] Aryastana, P., Ardantha, I. M., & Candrayana, K. W. (2018). Coastline change analysis and erosion prediction using satellite images. MATEC Web of Conferences, 197, 13003. doi:10.1051/matecconf/201819713003.

[6] Selamat, S. N., Abdul Maulud, K. N., Jaafar, O., & Ahmad, H. (2017). Extraction of shoreline changes in Selangor coastal area using GIS and remote sensing techniques. Journal of Physics: Conference Series, 852. doi:10.1088/1742-6596/852/1/012031.

[7] Darwish, K., & Smith, S. (2023). Landsat-Based Assessment of Morphological Changes along the Sinai Mediterranean Coast between 1990 and 2020. Remote Sensing, 15(5), 1392. doi:10.3390/rs15051392.

[8] El-Masry, E. A., Magdy, A., El-Gamal, A., Mahmoud, B., & El-Sayed, M. K. (2024). Multi-decadal coastal change detection using remote sensing: the Mediterranean coast of Egypt between El-Dabaa and Ras El-Hekma. Environmental Monitoring and Assessment, 196(2). doi:10.1007/s10661-024-12359-x.

[9] Abd-Elhamid, H. F., Zeleňáková, M., Barańczuk, J., Gergelova, M. B., & Mahdy, M. (2023). Historical Trend Analysis and Forecasting of Shoreline Change at the Nile Delta Using RS Data and GIS with the DSAS Tool. Remote Sensing, 15(7), 1737. doi:10.3390/rs15071737.

[10] Sanhory, A., El-Tahan, M., Moghazy, H. M., & Reda, W. (2022). Natural and manmade impact on Rosetta eastern shoreline using satellite Image processing technique. Alexandria Engineering Journal, 61(8), 6247–6260. doi:10.1016/j.aej.2021.11.053.

[11] Balbaa, S., El-gamal, A., Mansour, A. S., & Rashed, M. (2020). Mapping and Monitoring of Rosetta Promontory Shoreline Pattern Change, Egypt. Journal of Oceanography & Marine Environmental System, 4(2), 29–42. doi:10.5829/idosi.jomes.2020.29.42.

[12] Ghoneim, E., Mashaly, J., Gamble, D., Halls, J., & AbuBakr, M. (2015). Nile Delta exhibited a spatial reversal in the rates of shoreline retreat on the Rosetta promontory comparing pre- and post-beach protection. Geomorphology, 228(1), 1–14. doi:10.1016/j.geomorph.2014.08.021.

[13] Ali, E., Cramer, W., Carnicer, J., Georgopoulou, E., Hilmi, N. J. M., Le Cozannet, G., & Lionello, P. (2022). Cross-Chapter Paper 4: Mediterranean Region, Climate Change 2022: Impacts, Adaptation and Vulnerability. Contribution of Working Group II to the Sixth Assessment Report of the Intergovernmental Panel on Climate Change. IPCC, Cambridge, United Kingdom and New York, United States.

[14] Torresan, S., Furlan, E., Critto, A., Michetti, M., & Marcomini, A. (2020). Egypt's Coastal Vulnerability to Sea-Level Rise and Storm Surge: Present and Future Conditions. Integrated Environmental Assessment and Management, 16(5), 761–772. doi:10.1002/ieam.4280.

[15] El-Raey, M. (2010). Impacts and implications of climate change for the coastal zones of Egypt. Coastal Zones and Climate Change, 7, 31-50.

[16] El Sayed, W. R., Ali, M. A., Iskander, M. M., & Fanos, M. (2007). Evolution of Rosetta promontory during the last 500 years, Nile delta coast, Egypt. Eighth International Conference on the Mediterranean Coastal Environment (MEDCOAST), Alexandria, Egypt.

[17] Intergovernmental Panel on Climate Change (IPCC). (2022). Sea Level Rise and Implications for Low-Lying Islands, Coasts and Communities. The Ocean and Cryosphere in a Changing Climate, 321–446, Intergovernmental Panel on Climate Change (IPCC), Geneva, Switzerland. doi:10.1017/9781009157964.012.

[18] Glavovic, B., Dawson, R., Chow, W. T., Garschagen, M., Singh, C., & Thomas, A. (2022). Cities and settlements by the sea. Climate Change 2022 – Impacts, Adaptation and Vulnerability, 2163–2194, Cambridge University Press, Cambridge, United Kingdom. doi:10.1017/9781009325844.019.

[19] Elemam, D., & Eldeeb, A. (2023). Climate change in the coastal areas: consequences, adaptations, and projections for the Northern Coastal Area, Egypt. Scientific Journal for Damietta Faculty of Science, 12(2), 19–29. doi:10.21608/sjdfs.2023.170018.1061.

[20] Masria, A., Nadaoka, K., Negm, A., & Iskander, M. (2015). Detection of shoreline and land cover changes around Rosetta Promontory, Egypt, based on remote sensing analysis. Land, 4(1), 216–230. doi:10.3390/land4010216.

[21] Deabes, E. A. M. (2017). Applying ArcGIS to Estimate the Rates of Shoreline and Back-Shore Area Changes along the Nile Delta Coast, Egypt. International Journal of Geosciences, 8(3), 332–348. doi:10.4236/ijg.2017.83017.

[22] Fouad, W., Masria, A., Nassar, K., & Shamaa, M. T. (2020). Evaluation of the Rosetta Coastal Zone through Integration of Remote Sensing and Statistical Analysis (DSAS). International Journal of Scientific & Engineering Research, 11(9), 2020.

[23] Hemida, A. A., Khalifa, M., Abdelsalheen, M., & Afifi, S. (2023). A systematic review of coastal vulnerability assessment methods in the Egyptian context: the case study. HBRC Journal, 19(1), 161–181. doi:10.1080/16874048.2023.2241964.

[24] Fanos, A. M. (1999). Problems and protection work along the Nile delta coastal zone. Fifth International Conference on Coastal and Port Engineering in Developing Countries, 19-23 April, 1999, Cape-Town, South Africa.

[25] Frihy, O. E., & Lotfy, M. F. (1994). Mineralogy and textures of beach sands in relation to erosion and accretion along the Rosetta promontory of the Nile Delta, Egypt. Journal of Coastal Research, 10(3), 588–599.

[26] The Arab Contractors. (2010). Marine Protection of The Western Coast of Rosetta City – Egypt. The Arab Contractors, Cairo, Egypt. Available online: https://www.arabcont.com/English/project-370 (accessed on May 2024).

[27] Frihy, O. E., Shereet, S. M., & El Banna, M. M. (2008). Pattern of beach erosion and scour depth along the Rosetta promontory and their effect on the existing protection works, Nile Delta, Egypt. Journal of Coastal Research, 24(4), 857–866. doi:10.2112/07-0855.1.

[28] Explore Google Earth. (2024). Available online: https://earth.google.com/web (accessed on May 2024).

[29] USGS. (2024). EarthExplore: United States Geological Survey. Available online: https://earthexplorer.usgs.gov (accessed on May 2024).

[30] DSAS. (2024). Digital Shoreline Analysis System. Available online: https://code.usgs.gov/cch/dsas (accessed on May 2024).

[31] Aladwani, N. S. (2022). Shoreline change rate dynamics analysis and prediction of future positions using satellite imagery for the southern coast of Kuwait: A case study. Oceanologia, 64(3), 417–432. doi:10.1016/j.oceano.2022.02.002.

[32] Abd Wahid, M. Z. A., Osman, M. S., & Setumin, S. (2023). Comparative Analysis on Shoreline Changes in Kelantan, Malaysia Using Digital Shoreline Analysis System (DSAS). Esteem Academic Journal, 19(September), 109–117. doi:10.24191/esteem.v19iseptember.21031.

[33] Saad, R., Gerard, J. A., & Gerard, P. (2021). Detection of the shoreline changes using DSAS technique and remote sensing: a case study of Tyre Southern Lebanon. Journal of Oceanography and Marine Research, 9(11), 1000004.

[34] Gopinath, G., Thodi, M. F. C., Surendran, U. P., Prem, P., Parambil, J. N., Alataway, A., Al-Othman, A. A., Dewidar, A. Z., & Mattar, M. A. (2023). Long-Term Shoreline and Islands Change Detection with Digital Shoreline Analysis Using RS Data and GIS. Water (Switzerland), 15(2). doi:10.3390/w15020244.

[35] Song, Y., Shen, Y., Xie, R., & Li, J. (2021). A DSAS-based study of central shoreline changes in Jiangsu over 45 years. Anthropocene Coasts, 4(1), 115–138. doi:10.1139/anc-2020-0001.

[36] Himmelstoss, E. A., Henderson, R. E., Kratzmann, M. G., & Farris, A. S. (2018). Digital Shoreline Analysis System (DSAS) version 5.0 user guide. Open-File Report. doi:10.3133/ofr20181179.

[37] Zoysa, S., Basnayake, V., Samarasinghe, J. T., Gunathilake, M. B., Kantamaneni, K., Muttil, N., Pawar, U., & Rathnayake, U. (2023). Analysis of Multi-Temporal Shoreline Changes Due to a Harbor Using Remote Sensing Data and GIS Techniques. Sustainability (Switzerland), 15(9), 7651. doi:10.3390/su15097651.

[38] Singh, S., Singh, S. K., Prajapat, D. K., Pandey, V., Kanga, S., Kumar, P., & Meraj, G. (2023). Assessing the Impact of the 2004 Indian Ocean Tsunami on South Andaman's Coastal Shoreline: A Geospatial Analysis of Erosion and Accretion Patterns. Journal of Marine Science and Engineering, 11(6), 11. doi:10.3390/jmse11061134.